Hyperbranched Poly(ethylene glycol) Copolymers: Absolute Values of the Molar Mass, Properties in Dilute Solution, and Hydrodynamic Homology

ARTICLE *in* MACROMOLECULES · AUGUST 2015

Impact Factor: 5.8 · DOI: 10.1021/acs.macromol.5b01020

6 AUTHORS, INCLUDING:

Igor Perevyazko
Friedrich Schiller University Jena
19 PUBLICATIONS **153** CITATIONS
SEE PROFILE

Holger Frey
Johannes Gutenberg-Universität Mainz
364 PUBLICATIONS **10,404** CITATIONS
SEE PROFILE

Georges M Pavlov
Saint Petersburg State University
136 PUBLICATIONS **975** CITATIONS
SEE PROFILE

Macromolecules

Article

pubs.acs.org/Macromolecules

Hyperbranched Poly(ethylene glycol) Copolymers: Absolute Values of the Molar Mass, Properties in Dilute Solution, and Hydrodynamic Homology

Igor Perevyazko,[†,‡,⊥] Jan Seiwert,[§] Martina Schömer,[§] Holger Frey,[*,§] Ulrich S. Schubert,[*,†,‡] and Georges M. Pavlov[*,†,∥,⊥]

[†]Laboratory of Organic and Macromolecular Chemistry (IOMC) and [‡]Jena Center for Soft Matter (JCSM), Friedrich Schiller University Jena, Humboldtstrasse 10, 07743 Jena, Germany

[§]Institute of Organic Chemistry, Johannes Gutenberg-University, Duesbergweg 10-14, 55099 Mainz, Germany

[∥]Institute of Macromolecular Compounds, Russian Academy of Science, 199004 St. Petersburg, Russia

[⊥]Department of Molecular Biophysics and Polymer Physics, St. Petersburg State University, Universitetskaya nab. 7/9, 199034 St. Petersburg, Russia

Supporting Information

ABSTRACT: Hyperbranched poly(ethylene glycol) copolymers were synthesized by random anionic ring-opening multibranching copolymerization of ethylene oxide with glycidol as a branching agent, leading to poly(ethylene glycol) structure with glycerol branching points. Extending the available range of molar masses by novel synthesis strategies, a limited extent of control over the degree of polymerization was achieved by variation of the solvent in this copolymerization. Generally, absolute molar mass characterization of hyperbranched polymers still represents an unresolved challenge. A series of the hyperbranched poly(ethylene glycol)-*co*-(glycerol) copolymers (*hb*PEGs) of a wide range of molar masses ($1400 < M < 1\,700\,000$ g mol^{-1}), degree of branching (DB) = 0.04−0.54, and moderate polydispersity (M_w/M_n) ≈ 2.1 ± 0.2 were studied, in both water and dimethylformamide by the methods of molecular hydrodynamics. Analytical ultracentrifugation, intrinsic viscosity, translational diffusion measurements, and SEC were combined. Molar masses of *hb*PEGs were estimated from the comparison of the velocity sedimentation and translational diffusion coefficients, i.e., applying the Svedberg relationship. It was demonstrated that the use of linear PEG for the SEC calibration results in the significantly underestimated values of the molar masses of *hb*PEGs. The largest *hb*PEG samples exhibited a hydrodynamic radius of ≈14 nm in aqueous solution. The obtained Kuhn−Mark−Houwink−Sakurada scaling relations show linear trends in all range of molar masses. The detected scaling indexes virtually correspond to the homologous series characterized by a direct proportionality between the molar mass and the volume of the macromolecules that make up this series. The effect of branching on the molecular dimensions and on the hydrodynamic characteristics is discussed, and the corresponding contraction factors have been estimated.

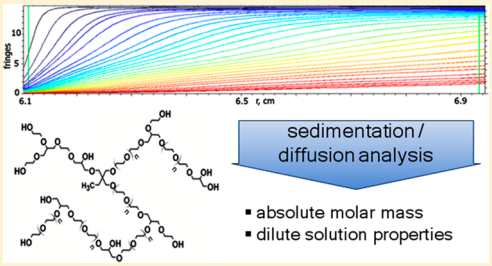

INTRODUCTION

Branched macromolecules with tree-like branching pattern play an important role in nature, where they perform a variety of essential functions, e.g., for energy storage and water retention. This class of polymers includes glycogen, amylopectin, dextran, glycoprotein complexes, and others. Their synthetic analogues were first studied in a systematic manner in the seminal works of Paul Flory.[1] The first actual syntheses of perfectly branched macromolecules, eventually called "dendrimers", were developed in the late 1970s and 1980s, capitalizing on both divergent and convergent construction approaches.[2−4] Dendrimers have attracted wide attention due to their unique branch-on-branch topology, compact structure, and large number of end groups available for further modification. However, in recent years, motivated by the demanding multistep synthesis of dendrimers, the attention of researchers has turned to "one-pot" strategies, resulting in hyperbranched macromolecules that exhibit unique characteristics that are a consequence of their particular topology and high branching density.[5−12] However, hyperbranched polymers based on multifunctional AB_2 polycondensation show large heterogeneity with respect to both molar masses and branching.[8,13−15] An important strategy to overcome these drawbacks relies on the slow addition of reactive AB_2 monomers onto a core, permitting to reduce the dispersity and enabling a certain extent of control over molar mass.[16,17]

Despite the enormous advances in this area, absolute molar mass characterization for hyperbranched polymers is still an

Received: May 13, 2015
Revised: July 31, 2015

DOI: 10.1021/acs.macromol.5b01020
Macromolecules XXXX, XXX, XXX−XXX

unresolved issue. Although several efforts have been reported in this direction and theoretical considerations have been published, in addition no suitable theory exists to describe the solution behavior of the different branched polymers.[18−25] In particular, it is still unclear whether hyperbranched polymers will follow the well-known scaling relationships between hydrodynamic characteristics ($P_i = K_{ij}P_j^b$, where P_i is one of the hydrodynamic characteristics $[\eta]$, D_0, s_0, k_s, f/f_{sph} and P_j is another hydrodynamic characteristic from this row or molar mass) and, as a consequence, whether they can be considered as fractal or self-similar structures. Furthermore, the conformation of these macromolecules in solution is still an open issue.

In this contribution, on the one hand, we demonstrate that by variation of the solvent used for the synthesis a broad range of molar masses of the hyperbranched poly(ethylene glycol) copolymers becomes available. On the other hand, we report the results of a study of a series of such nonfractionated hyperbranched poly(ethylene glycol)-*co*-poly(glycerol) copolymers ("hyperbranched PEG", *hb*PEG) copolymers with glycerol units as branching points, encompassing a wide range of molar masses. The materials were synthesized by the random anionic ring-opening copolymerization of ethylene oxide with glycidol as a branching agent, as introduced in a recent communication (Scheme 1).[26] Linear PEG is the gold-

Scheme 1. Synthesis of *hb*PEG by Random Anionic Ring-Opening Copolymerization of Ethylene Oxide and Glycidol[a]

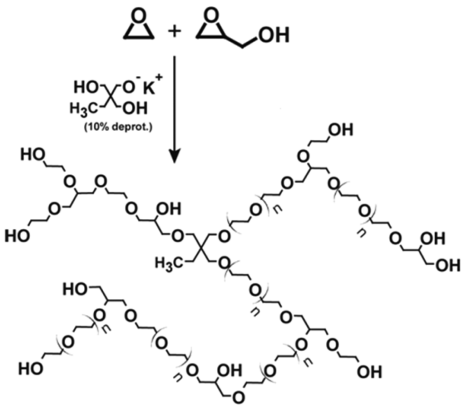

[a]The ratio of epoxide comonomers determines the degree of branching.

standard biomedical polymer because of its outstanding biocompatibility and solubility in both water and polar organic solvents.[27−29] Hyperbranched PEG copolymers combine these remarkable properties with a dendritic structure, which impedes or even prevents crystallization and provides multiple functional groups for further functionalization.[17,30−33] Contrary to other strategies for the synthesis of branched PEG analogues,[34−44] *hb*PEG is obtained in a convenient one-step batch polymerization with full conversion, resulting in a purely aliphatic polyether structure (Scheme 1). The resulting *hb*PEGs exhibit high molar masses and moderate apparent dispersities in the range of 1.1−1.7, as determined by size-exclusion chromatography (SEC).[24] However, reliable results concerning absolute molar masses cannot be obtained by this relative method. We have therefore chosen to investigate the copolymers by the methods of molecular hydrodynamics, in particular by analytical ultracentrifugation, intrinsic viscosity measurements, translation diffusion, and SEC measurements, for comparison. We focus on the properties of dilute solutions of the hyperbranched PEG copolymers, aiming at the effect of branching on the molecular characteristics and the conformation of the macromolecules.

To the best of our knowledge, ultracentrifugation has hardly been employed for the study of hyperbranched polymers up to date.[45] Here we introduce new synthetic strategies permitting to obtain *hb*PEG with different molar masses. In the ensuing sections we discuss the basic hydrodynamic data: (i) molar mass, (ii) scaling relationships, (iii) branching factors, and (iv) global conformation of the hyperbranched polyethers.

EXPERIMENTAL PART

Analytical Ultracentrifugation (AUC) and Translation Diffusion. Sedimentation velocity experiments were performed with a ProteomeLab XLI Protein Characterization System analytical ultracentrifuge (Beckman Coulter, Brea, CA), using conventional double-sector Epon or aluminum centerpieces of 12 mm optical path length and a four-hole rotor (AN-60Ti). Rotor speed was 40 000−60 000 rpm, depending on the sample. Cells were filled with 420 μL of sample solution and 440 μL of solvent (water or dimethylformamide (DMF)). Three concentrations of each sample in H_2O and in DMF were studied, covering a wide concentration range ($3 \leq c_{max}/c_{min} \leq 7$). The parameter $c[\eta]$ characterizing the degree of dilution was in the range $0.002 \leq c[\eta] \leq 0.038$, corresponding to a very high dilution state. This, in turn, allows for reliable extrapolation to concentration zero (c: polymer concentration in g cm^{-3}; $[\eta]$: intrinsic viscosity, measured in cm^3 g^{-1}). Before the run, the rotor was equilibrated for approximately 1 h at 20 °C in the centrifuge. Sedimentation profiles were obtained at the same temperature, using interference optics. For the analysis of the sedimentation velocity data, *ls*-$g^*(s)$ and $c(s)$ with a Tikhonov−Phillips regularization procedure implemented into the Sedfit program were applied.[46] The *ls*-$g^*(s)$ model represents a least-squares boundary analysis which describes sedimentation of nondiffusing species. The $c(s)$ analysis is based on the numerical resolution of the Lamm equation assuming the same frictional ratio (f/f_{sph}) values for each sedimenting species. The velocity sedimentation coefficients (s) were extrapolated to zero concentration by linear approximation, following the relationship $s^{-1} = s_0^{-1}(1 + k_s c)$, where s_0 is the extrapolated value of the velocity sedimentation coefficient and k_s is the concentration sedimentation coefficient (Gralen coefficient).

The translation diffusion coefficients D_0 were estimated in water by the classical method of forming, in the analytical ultracentrifuge at low speed rotation (n = 3000 rpm), a solution−solvent boundary using synthetic boundary cells.[47] The diffusion interferograms were processed by the maximal ordinate and area method.[48] The diffusion coefficient D_0 was calculated from the slope of the experimental dependence of the dispersion σ^2 (cm^2) of the diffusion boundary on time (Figure 1).

$$D = \frac{\Delta\sigma^2}{2\Delta t} \quad (1)$$

Viscosity Measurements. Viscosity measurements were conducted using an AMVn viscometer (Anton Paar, Graz, Austria), with a capillary/ball combination of the measuring system. The respective flow times for the solvent and polymer solutions, τ_0 and t, were measured at 20 °C, with relative viscosities $\eta_r = t/t_0$ in the range of 1.2−2.5, which corresponds to dilute solutions. The extrapolation to zero concentration was achieved by using both the Huggins [$(\eta_r - 1)/c = [\eta] + k_H[\eta]^2c + ...$, where k_H is the Huggins parameter and c is the concentration] and the Kraemer equations [$(\ln \eta_r)/c = [\eta] + k_K[\eta]^2c + ...$, where k_K is the Kramer parameter], and the average values were considered as the value of the intrinsic viscosity ($[\eta]$, cm^3 g^{-1}).

Partial Specific Volume Determination. The density measurements were carried out in the density meter DMA 02 (Anton Paar, Graz, Austria) according to the procedure of Kratky et al.[49]

DOI: 10.1021/acs.macromol.5b01020
Macromolecules XXXX, XXX, XXX−XXX

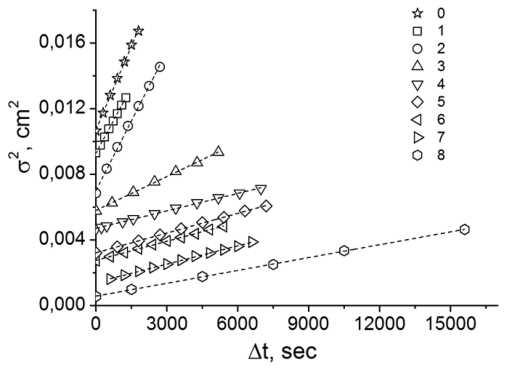

Figure 1. Dependence of the diffusion dispersion σ on the time t for the hyperbranched PEG copolymers in water. For other properties of samples 0–8, see Tables 1–3.

NMR Spectroscopy. ^{1}H NMR and ^{13}C NMR spectra were recorded at 400 and 100 MHz, respectively, on a Bruker AMX400 apparatus and were referenced internally to residual signals of the deuterated solvent.

Size-Exclusion Chromatography (SEC). For SEC measurements in DMF (containing 0.25 g L^{-1} of lithium bromide as an additive), an Agilent 1100 series was used as an integrated instrument including a PSS HEMA column ($10^6/10^4/10^2$ Å porosity) and UV and RI detector. As the first step calibration was carried out with *linear* poly(ethylene glycol) standards provided by Polymer Standards Service (PSS). Because of the completely different hydrodynamic behavior of linear PEG standards compared to highly branched PEG copolymers, in this case, SEC is considered only as a qualitative method to obtain basic information regarding the differences between the synthesized samples according to their elution volume. For the quantitative estimates the columns were calibrated with the molar masses obtained from the sedimentation-diffusion analysis of the samples.

Materials. All reagents and solvents were used as received, if not otherwise mentioned. Ethylene oxide (EO) and glycidol were dried over calcium hydride (CaH_2) and distilled under vacuum directly prior to use. Tetrahydrofuran (THF) was purified by vacuum distillation over sodium/benzophenone.

Synthesis of the *hb*PEG Polymers. A two-necked glass flask equipped with a septum, Teflon seal, and a magnetic stirrer was connected to a vacuum line. 44 mg (0.33 mmol, 1.0 equiv) of 1,1,1-tris(hydroxymethyl)propane (TMP) was mixed with 0.10 mL (0.10 mmol, 0.3 equiv) of potassium *tert*-butoxide (1 M solution in THF) to deprotonate 10% of the hydroxyl groups. 5 mL of benzene was added to the resulting slurry and stirred for 30 min, and the flask was evacuated for at least 4 h to remove traces of water azeotropically as well as other volatiles. In contrast to previous syntheses,[24] different solvents were employed to increase or lower the molar mass of the resulting polymers. For the synthesis of *hb*PEG oligomers and low molar mass polymers, the deprotonated initiator was dissolved in 5 mL of dry dimethyl sulfoxide (DMSO). High molar mass copolymers were obtained by using 20 mL of dioxane or THF as an emulsifying solvent. In both cases a total amount of 100 mmol (300 equiv) monomer was transferred to the reaction vessel, systematically varying the comonomer ratio to obtain a series of hyperbranched copolymers with different degree of branching (DB). Ethylene oxide (40–95 mmol) was transferred to an ampule, dried over calcium hydride, and subsequently transferred to the reaction flask under vacuum. The flask was sealed with a septum, and glycidol (60 to 5 mmol) was introduced through the septum via cannula. The reaction mixture was then immediately heated to 80 °C and stirred for 18 h. After completion of the reaction, methanol was added, and the solution was neutralized by filtration over an acidic cation exchange resin (DOWEX WX8). The resulting *hb*PEG polymers were precipitated in cold diethyl ether. In the case of the high molar mass polymers the products were dialyzed against methanol (MWCO 3000 g mol^{-1}). All products were dried under vacuum overnight at 85 °C (yield 80–90%).

Caution: In very few cases the pressure evolving in the early stages of the reaction in the flask led to the spontaneous removal of the septum and release of ethylene oxide. Thus, the reaction has to be carried out in an appropriate fume hood, and the respective safety precautions should be taken. In general, the amount of EO used did not exceed 10 g per batch in a 250 mL flask to guarantee a safe reaction.

^{1}H NMR (DMSO-d_6, 400 MHz): δ (ppm) = 4.81–4.35 (m, br, OH); 4.10–3.06 (m, O–CH, O–CH_2); 1.36–1.18 (m, 2H, CH_3–CH_2 (TMP)); 0.89–0.68 (m, 3H, CH_3 (TMP)). ^{13}C NMR (DMSO-d_6, 100 MHz): δ (ppm) = 80.25–79.45 (m, linear$_{G13}$ CH); 78.52–77.42 (m, dendritic$_G$ CH); 73.22–72.10 (m, 2 linear$_{G14}$ CH_2); 72.04–69.62 (m, 2 dendritic$_G$ CH_2, 2 linear$_E$ CH_2, terminal$_E$ CH_2–CH_2–OH, terminal$_G$ CH, terminal$_G$ CH_2); 69.61–68.37 (m, linear$_{G13}$ CH_2, linear$_{G14}$ CH–OH); 63.39–62.96 (terminal$_G$ CH_2–OH); 60.87–60.07 (m, terminal$_E$ CH_2–OH, linear$_{G13}$ CH_2–OH).

RESULTS AND DISCUSSION

Synthesis and NMR/SEC Characterization. In the first communication on the polymerization of *hb*PEG, copolymers with apparent molar masses in the range of 23 000–50 000 g mol^{-1} were described, as determined by SEC calibrated with linear PEG standards, focusing on the control over the glycidol content and the degree of branching.[26] A detailed study of solvent effects in the current work made it possible to expand the synthetic strategy toward both higher and lower molar masses, as shown below. The degree of polymerization was found to be largely independent of the monomer ratio EO/glycidol. Unfortunately, the slow monomer addition strategy that was established for glycidol homopolymerization[29] was not applicable in this case due to the low boiling point of EO. One-pot synthesis leads to an increased extent of autoinitiation processes, i.e., glycidolate formed by proton transfer during polymerization. This originates from the fast proton transfer from excess glycidol to a TMP anion. Hence, after separating low molecular byproducts from the polymer during work-up, NMR studies revealed significant amounts of unreacted initiator.

Since the previously reported procedure for the synthesis of hbPEG always afforded (apparent) molar masses of 23 000–50 000 g mol^{-1} (SEC using PEG standards), both THF and dioxane have been explored as emulsifying agents for the copolymerization. The *hb*PEG samples with apparent molar masses up to 65 000 g mol^{-1} (SEC) and mostly narrow, monomodal molar mass distribution were obtained (Table 1). This is in analogy to the approach introduced by Brooks et al., who obtained narrowly distributed, high molar mass hyperbranched polyglycerol (*hb*PG) with apparent M_n (SEC) up to 700 000 g mol^{-1} using dioxane as a cosolvent.[50] The authors explained the unexpectedly high degree of polymerization with an accelerated proton transfer caused by the apolar medium and incomplete conversion of the initiator. Accordingly, for *hb*PEG as well as *hb*PG a small amount of a low molar mass fraction was obtained that could be removed from the polymer by dialysis. In either case, neither the initiator nor the growing polymer is completely soluble in these solvents; i.e., the reaction can be viewed as an emulsion-like process. Surprisingly, although *hb*PEG **3** was prepared in the same manner, it exhibited a significantly lower molar mass of only 14 400 g mol^{-1} (SEC) and the broadest molecular weight distribution of all samples. Nevertheless, its solution properties were studied, despite the high dispersity of this sample, as no

DOI: 10.1021/acs.macromol.5b01020
Macromolecules XXXX, XXX, XXX–XXX

Table 1. NMR and SEC Characterization Data for *hb*PEG with Varying Monomer Composition, Prepared in DMSO (Samples 0–2) and THF/Dioxane (Samples 3–8)

no.	G% (^{13}C)	DB (^{13}C)	M_n[a] (g mol^{-1})	PDI[a]	M_n[b] (g mol^{-1})	PDI[b]	peak vol (cm^3)
0	33	0.36	880	1.39	300	5.03	22.55
1	14	0.13	1600	1.29	1300	2.87	21.38
2	7	0.04	2480	1.28	3200	2.71	20.28
3	54	0.54	14400	1.69	57000	5.83	17.41
4	7	0.07	36000	1.26	440000	2.58	14.05
5	34	0.37	40400	1.33	530000	2.00	14.01
6	29	0.29	55300	1.04	1450000	1.16	13.79
7	64	0.53	64600	1.02	1600000	1.10	13.78
8	16	0.16	65300	1.07	1700000	1.28	13.75

[a]Apparent values of M_n and PDI (= M_w/M_n) obtained by calibration with linear PEG standards. [b]Calculated based on the columns calibration with the molar masses obtained from AUC.

other polymers in the molar mass range between 3000 and 20 000 g mol^{-1} (SEC) were obtained under the conditions explored.

In contrast, copolymerization of ethylene oxide and glycidol in DMSO was generally found to lead to the formation of oligomers and low molar mass polymers in the range of 500–3000 g mol^{-1} (M_n, apparent molar mass, SEC; samples 0–2 in Table 1) with moderate polydispersities between 1.3 and 1.4 after purification by precipitation in diethyl ether. Because of the polar solvent, the initiator is dissolved completely, and presumably chain transfer from polymer to monomer occurs with higher frequency, since the anion solvation is better than in THF/dioxane. DMSO provides better complexation of the cation, and as a stronger Lewis base it polarizes the oxygen–hydrogen bond more strongly.

Determination of the degree of polymerization via ^{1}H NMR spectroscopy, as often used in the case of hyperbranched polyglycerol, was not feasible, since full incorporation of the initiator into each macromolecule is a prerequisite for this characterization technique. Even complete conversion, however, would not permit characterization for a molar mass beyond a few thousand g mol^{-1}, as the initiator to monomer ratio is so low that the corresponding proton signal cannot be distinguished in the spectra. Characterization of the copolymers in this molar mass range by MALDI-TOF mass spectrometry is not possible either. However, both the ratio of incorporated monomers and the relative amounts of branched, linear, and terminal units can be calculated from inverse gated ^{13}C NMR spectra, as described previously.[26] The signal splitting due to triad sequences allows for determining the relative amount of branched, linear, and terminal units as well. From these, the degree of branching (DB) was calculated as defined by eq 2.[51]

$$\mathrm{DB}_{\mathrm{AB/AB_2}} = \frac{2D}{2D + L_{co}} \tag{2}$$

D summarizes all dendritic units, whereas L_{co} summarizes all linear units in the hyperbranched copolymers. AB represents a monomer unit containing two reactive sites, in this case ethylene oxide, and AB_2 represents the branching unit glycidol as a latent AB_2 monomer. Assuming equal reactivity of all B groups and full conversion, the theoretical DB of an AB/AB_2 copolymer with the comonomer ratio r (x_{AB}/x_{AB_2}; initial comonomer ratio) can be obtained from eq 3 for comparison, provided all B groups possess reactivity (Figure 2).[51]

$$\mathrm{DB}_{\mathrm{AB/AB_2,theo}} = 2\frac{r+1}{(r+2)^2}, \quad \text{with } r = \frac{x_{AB}}{x_{AB_2}} \tag{3}$$

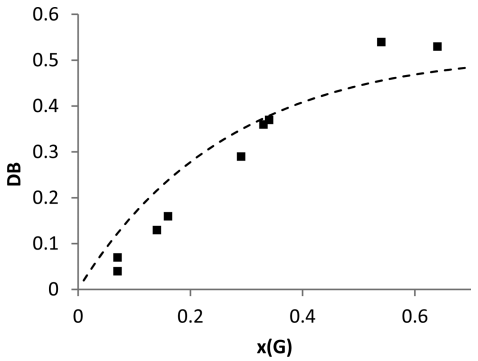

Figure 2. Experimentally determined degree of branching of *hb*PEG with varying monomer composition as a function of the glycidol mole fraction. The dashed line represents theoretical values calculated from eq 3.

SEC and NMR data are given in Table 1. The SEC peak volume is included for the ensuing discussion. Summarizing the results, the lack of control over the molar mass for the copolymerization of ethylene oxide and glycidol in bulk has been overcome to a certain extent by modifying the existing reaction protocol. While still obtaining relatively moderate PDI values (Table 1), the use of polar aprotic solvent led to the formation of oligomers. On the other hand, carrying out the polymerization in cyclic ethers increased apparent molar masses (SEC) up to 65 000 g mol^{-1}.

3.2. Hydrodynamic Characterization. *3.2.1. Discussion of Experimental Data That Generally Do Not Depend on Molar Mass. Primary Experimental Data.* First, we discuss those experimental data and their combinations that typically do not depend on the molar mass. Other data allow calculation of the molar mass of the substances dispersed in the solvent and evaluation of their hydrodynamic size and shape. Note that the former data are important for the characterization of polymers in solution and, as a rule, are used for the homologous series of linear polymers; moreover, these data are usually included in the summary tables in various polymer handbooks.[52] For branched polymer systems, the definition "homologous" in its standard meaning cannot be applied due to the absence of uniform structural repeating units in the polymer. However, it seems worth testing how those values which are virtually constant for linear polymers will depend on the molar mass/composition for the particular case of hyperbranched poly(ethylene glycol)-*co*-poly(glycerol) copolymers.

Partial Specific Volume and Refractive Index Increment. The partial specific volume υ (cm^3 g^{-1}) was calculated from the corresponding density increment measurements as $\Delta\rho/\Delta c = 1 - \upsilon\rho_0$, where ρ_0 is the density of the solvent, for all samples in water and DMF (values are given in Table 2).

The values of the refractive index increment were evaluated from the sedimentation velocity data as follows:

$$\frac{\mathrm{d}n}{\mathrm{d}c} = \frac{J}{c}\frac{\lambda}{kl} \tag{4}$$

DOI: 10.1021/acs.macromol.5b01020
Macromolecules XXXX, XXX, XXX–XXX

Table 2. Intrinsic Viscosity ($[\eta]$, cm^3 g^{-1}), Huggins (k_H), and Kraemer (k_K) Parameters and Values of Partial Specific Volume (υ, cm^3 g^{-1}) for All *hb*PEG Samples in Water and DMF[a]

no.	$[\eta]_{water}$	k_H	k_K	$[\eta]_{DMF}$	k_H	k_K	υ_{water}	υ_{DMF}
0				4.9	0.88	0.06		0.825
1	6.2	0.84	0.03	5.9	0.78	0.02	0.840	0.840
2	5.9	0.62	0.02	6.0	0.61	−0.04	0.817	0.853
3	6.5	1.79	0.53	6.9	1.23	0.26	0.787	0.792
4	7.3	2.03	0.50	6.8	2.33	0.44	0.829	0.857
5	5.7	2.40	0.52	6.3	1.14	0.22	0.802	0.813
6	5.6	2.05	0.50	5.7	1.76	0.35	0.772	0.810
7	5.5	1.59	0.42	6.5	0.77	0.03	0.769	0.760
8	7.9	1.78	0.32	7.1	1.65	0.33	0.813	0.857

[a]Average values of the partial specific volume of *hb*PEG are $\upsilon = 0.804 \pm 0.03$ cm^3 g^{-1} and $\upsilon = 0.82 \pm 0.04$ cm^3 g^{-1} in H_2O and DMF, respectively. It should be noted that these values of the partial specific volume generally decrease somewhat with increasing glycerol fraction (Figure 2). This trend is more pronounced in DMF than in water. Consequently, for all corresponding calculations the individual values of υ were used.

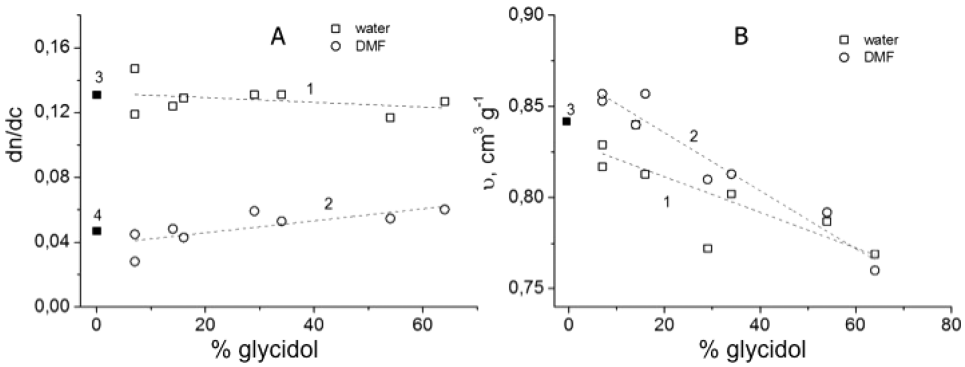

Figure 3. Correlation of (A) the refractive index increment dn/dc (cm^3/g) and (B) the partial specific volume υ (cm^3/g) on the glycidol content (%) in the *hb*PEG macromolecules. 1: in water; 2: in DMF; 3: value for linear PEG in water; 4: value for linear PEG in DMF (*Polymer Handbook*[52]).

where J is the number of interference fringes, λ is the wavelength used (655 nm), l is the optical path length (12 mm), and k is a device constant.

In water, the values of the refractive index increment of *hb*PEG are virtually independent of the glycerol content for the high molar mass samples (M > 100 000 g mol^{-1}), and the average value of dn/dc is 0.126 ± 0.003 cm^3 g^{-1}. In DMF the dn/dc values increase slightly with increasing glycidol content (Figure 3), and the average values are lower in comparison to the aqueous solutions (dn/d$c^{av} \approx 0.053$). This difference in dn/dc is mainly due to the difference in the refractive indices of the solvents (n_{DMF} = 1.427 and n_{H_2O} = 1.333). The linear approximation for the dn/dc dependence of the glycidol content in DMF is characterized by a low coefficient of the linear correlation and cannot be used to determine the proportion of glycidol in the copolymer. In contrast, the dependencies of the partial specific volume vs glycidol content are more pronounced, have a palatable quality of the linear fit, and can be used in principle for the evaluation of the glycidol content in copolymers. The following dependences of υ in both solvents $\upsilon = 0.831 - 0.977 \times 10^{-3}$ G% (r = 0.8088) and $\upsilon = 0.867 + 1.590 \times 10^{-3}$G% ($r$ = 0.9689) in water and DMF were obtained, respectively. The results obtained by densitometry indicate that the value of the partial specific volume may be used for the approximate estimation of the glycerol content in the samples and, thus, the degree of branching of the macromolecules.

Ratio of k_s/[η]. The dimensionless ratio $\gamma = k_s/[\eta]$, of the concentration dependence coefficient k_s (Gralen coefficient) on the intrinsic viscosity $[\eta]$,[53] depends on the particle/macromolecule asymmetry/conformation; the value for coils of linear macromolecules is ≈1.7 with the general tendency to decrease for more rigid macromolecules and to increase for compact, globular molecules.[53−55] The average values obtained for *hb*PEG samples are γ = 2.9 ± 0.5 and 4 ± 2 for water and DMF solutions, respectively. Remarkably, these values are close to the theoretically predicted value for rigid spheres: $(k_s/[\eta])_{sph}$ = 2.75.

Huggins and Kraemer Parameters. The viscometric Huggins parameter (k_H) usually varies from 0.3 to 0.5 for linear polymers, and the Kraemer parameter (k_K) is usually negative. For the *hb*PEG copolymers of high molar mass (M > 100 000 g mol^{-1}), the k_H and k_K values fluctuate around the averages which are in H_2O (k_H^{av} = 1.9 ± 0.1, k_K^{av} = +(0.47 ± 0.03)) and in DMF (k_H^{av} = 1.5 ± 0.2, k_K^{av} = +(0.27 ± 0.06)). These values are typical for compact macromolecules in solution. For rigid spheres k_H^{sph} is 2.26.[56]

Hydrodynamic Invariants. The intercorrelation between the basic hydrodynamic characteristics ($[\eta]$, s_0, D_0, $(f/f_{sph})_0$) can be evaluated by calculating the hydrodynamic invariants A_0 ([g cm^2 s^{-2} K^{-1} mol$^{-1/3}$]) and β_s ([mol$^{-1/3}$]), which remain virtually independent of molar mass for linear homologous series.[57,58]

$$A_0 = (R[s][D]^2[\eta])^{1/3} \quad (5)$$

$$\beta_s = k_B^{-2/3}(N_A[s][D]^2 k_s)^{1/3} \quad (6)$$

where k_B is the Boltzmann constant, R is the gas constant, N_A is Avogadro's number, $[s]$ is the intrinsic sedimentation coefficient ($[s] = s_0\eta_0/(1 - \upsilon\rho_0)$), $[D] = D_0\eta_0/T$ is the

DOI: 10.1021/acs.macromol.5b01020
Macromolecules XXXX, XXX, XXX−XXX

Table 3. Hydrodynamic Characteristics, Molar Masses, and Hydrodynamic Invariants of Hyperbranched PEG Copolymers in Water at 20 °C

no.	glycidol content (%)	s_0 (S)	k_s (cm^3 g^{-1})	$k_s/[\eta]$	$D \times 10^7$ (cm^2 s^{-1})	$(f/f_{sph})_0$	M_{av}[a] $\times 10^{-3}$ (g mol^{-1})	PDI[b]	$A_0 \times 10^{-10}$	$\beta \times 10^7$
0	33				32.3		1.4	2.02		
1	14	0.16	20	3.2	13.8	1.91	2.2	2.20	2.27	1.13
2	7	0.20	21	3.6	13.5	2.03	2.0	2.42	2.25	1.15
3	54	3.36	21	3.2	3.29	2.36	130	3.30	2.20	1.09
4	7	9.97	23	3.2	1.78	2.75	1000	2.01	2.32	1.14
5	34	10.8	14	2.5	2.00	2.80	800	1.77	2.42	1.10
6	29	15.0	14	2.5	1.88	2.93	1500	1.75	2.34	1.07
7	64	17.6	18	3.3	1.82	2.44	1000	1.37	2.46	1.23
8	16	20.1	16	2.1	1.30	1.95	1700	2.07	2.43	1.03

[a]Average values of the molar masses are obtained as $M_{av} = (M_{sD}^{H_2O} + M_{sf}^{H_2O} + M_{sf}^{DMF})/3$ with the average relative error 23%. [b]Calculated from the sedimentation velocity data.

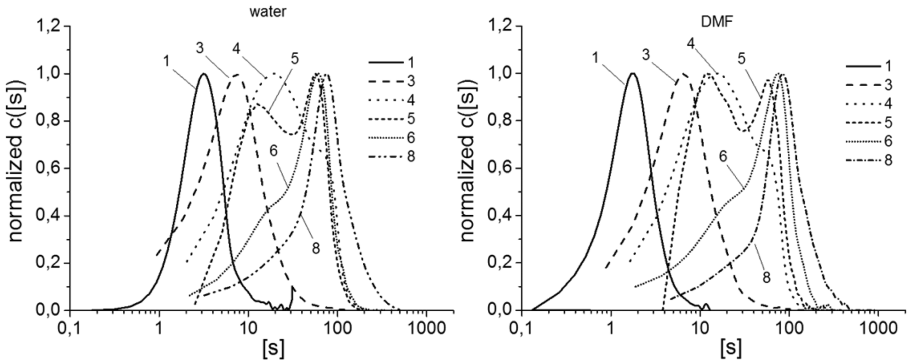

Figure 4. Semilogarithmic plot of the differential distributions of intrinsic sedimentation coefficients of hyperbranched PEG copolymers in water, as obtained by the Sedfit software ($c(s)$ analysis); left: samples in water; right: in DMF.

intrinsic diffusion coefficient, ρ_0 and η_0 are density and dynamic viscosity of the solvent, and T is the temperature (in K).

The average value of A_0 is 3.2×10^{-10} for linear flexible chain polymers and 3.8×10^{-10} for rigid chain molecules; the minimum theoretically predicted value for rigid spheres is 2.914×10^{-10}.[57] In the current case the average value of A_0 was calculated to be $(2.35 \pm 0.10) \times 10^{-10}$ and $(2.50 \pm 0.40) \times 10^{-10}$ for samples in water and DMF, respectively. Systematic observations on the hydrodynamic invariants for highly branched macromolecular systems have been published only for perfect dendrimers, i.e., poly(amidoamine) and poly(propyleneimine) to date.[59−65] The overall average value obtained for different dendrimer generations with up to 128 end groups is $A_0^{av} = (2.53 \pm 0.05) \times 10^{-10}$, which correlates with the values obtained for *hb*PEG copolymers obtained in the current study. It should be noted that the values of A_0 for highly branched macromolecules are generally lower than the theoretical value for rigid spheres. At the same time, the obtained values of the sedimentation parameter $\beta_s = (1.13 \pm 0.06) \times 10^7$ and $(1.09 \pm 0.10) \times 10^7$ in water and DMF, respectively, are in the range known from the literature for linear chain polymers.[66]

Discussion: Basic Hydrodynamic Characteristics and Branching Factors of hbPEG; Molar Mass, Hydrodynamic Homology, and Kuhn−Mark−Houwink−Sakurada Relationships. The basic hydrodynamic characteristics are s_0, D_0, and $[\eta]$. These values are related to the molar mass, size, and shape of the dissolved species. The values of the molar mass were calculated based on the coefficients s_0 and D_0 using the Svedberg equation (eq 5):

$$M_{sD} = \frac{s_0 RT}{D_0(1 - \upsilon\rho_0)} \tag{7}$$

Alternatively, it was based on s_0 and $(f/f_{sph})_0$ coefficients using a modified Svedberg equation:

$$M_{sf} = 9\pi\sqrt{2}N_A([s]f/f_{sph})^{3/2}\sqrt{\upsilon} \tag{8}$$

In the following discussion, the average values of the molar masses will be used:

$$M_{av} = (M_{sD}^{H_2O} + M_{sf}^{H_2O} + M_{sf}^{DMF})/3 \tag{9}$$

The molar mass values, together with other hydrodynamic characteristics in H_2O, are summarized in Table 3; the data obtained in DMF are presented in the Supporting Information (Table 1).

The absolute values of the molar masses evaluated from the sedimentation-diffusion analysis allow to make the appropriate calibration of the SEC columns. Such SEC calibrations provide the adequate values of the molar mass (compare data in Tables 1 and 3).

Figure 4 compares differential distributions of the intrinsic sedimentation coefficients $[s]$ of *hb*PEG in water and DMF. The two distributions are virtually identical. Notably, the distributions shift to higher values of the sedimentation coefficients with increasing molar mass. Moreover, the distributions in general are broad which, in turn, reflects the high polydispersity/heterogeneity of the samples. In addition, it is obvious that at some point (sample 4) a second component in a higher molar mass region appears. In the following, the distribution becomes strictly bimodal (sample 5); afterward, the

DOI: 10.1021/acs.macromol.5b01020
Macromolecules XXXX, XXX, XXX−XXX

low molar mass component decreases (sample 6), and the distribution again becomes unimodal (sample 8). Since the samples are unfractionated, such a behavior is most probably related to inhomogeneous structures of the respective samples.

The SEC data (Figure 5) do not provide such a clear tendency toward the existence of several species in the solution.

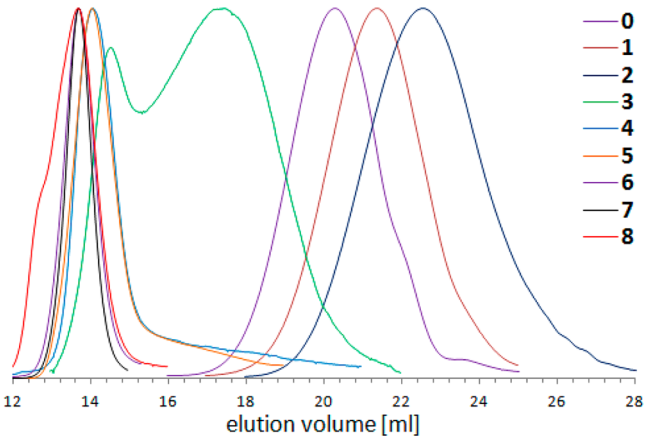

Figure 5. SEC traces (DMF, RI signal) of the hyperbranched PEG copolymers.

They show, however, the presence of a shoulder/wide tail for samples 4 and 5; moreover, a clear bimodal distribution was obtained for sample 3.

The polydispersity can also be evaluated from the sedimentation velocity data by transforming the initial distribution of sedimentation coefficients into the distribution by the molar masses. The PDI can be then calculated based on the known relationships: $M_n = \sum_i N_i M_i / N_i$, $M_w = \sum_i N_i M_i^2 / \sum_i N_i M_i$. The calculated values are listed in Table 3. The differences in the distributions obtained by analytical ultracentrifugation and SEC could be related to the fact that the AUC is more sensitive in the range of high molar mass, and SEC is more sensitive in the range of the low molar mass polymers. A detailed discussion regarding the analysis of the differences in the distributions obtained by SEC on one side, and AUC on another one will be made in a future publication.

Comparison of the basic experimental characteristics s_0, D_0, and $[\eta]$ shows that the value of $[\eta]$ fluctuates around its average, while the values of s_0 increase by 2 and the D_0 values decrease by 1 order of magnitude when going from sample 1 to sample 8.

The *hb*PEG samples can be qualitatively assigned to the most probable conformation by comparing their hydrodynamic volumes with the corresponding molar masses.[67,68] The $[\eta]M$ is the key value in interpreting the results of size exclusion chromatography of polymers (Benoit universal calibration).[69] It is proportional to the volume V occupied by the macromolecules in solution. In the first approximation, the slope of the $[\eta]M$ dependency on molar masses, in a double-logarithmic scale, will be inversely proportional to the average intracoil density ($\sim \log(1/\rho)$). The higher the curves are located along the ordinate, the lower will be the density of the polymer substance in the volume occupied by the polymer molecule. Figure 6 shows that the data obtained for *hb*PEG virtually coincide with the average dependence obtained for dendrimers, but also glycogen and globular proteins, where the slope is equal to 1. This means that the volume occupied by the

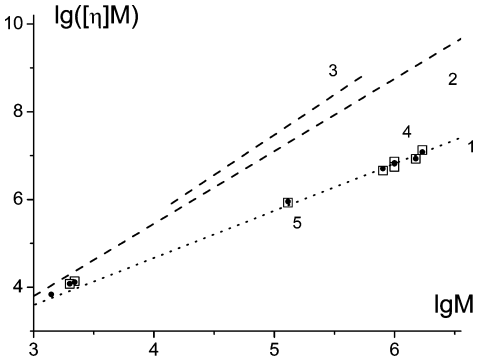

Figure 6. Dependence of the hydrodynamic volume $[\eta]M$ on M, in a double-logarithmic plot. The dotted line 1: completely compact organization of the polymer species inside the occupied volume (similar to glycogen, dendrimers, globular proteins); dashed line 2 corresponds to the behavior of linear PEG (flexible linear macromolecules); the dashed line 3 describes the behavior of rigid linear macromolecules (polysaccharides schizophyllan[72] and xanthan[73]); points corresponding to the studied *hb*PEG macromolecules (4) in H_2O and (5) in DMF (see also Tables 2 and 3).

macromolecules (V) is directly proportional to their molar mass: $V \sim M$ and, consequently, the intrinsic viscosity values are virtually independent from M, since $[\eta] = 6^{3/2}\Phi(\langle R_g^2\rangle^{3/2}/M)$, where Φ is the Flory hydrodynamic parameter and R_g is the radius of gyration.

Homology of linear macromolecules is provided by the constant chemical structure of the repeating units, and persistence of a structural parameter—linear density of the polymer chains M_L—can be defined as a *structural homology*. Homology of branched macromolecules, in particular hyperbranched copolymers, is more difficult to define and much more difficult to achieve and control. Here we propose the concept of *hydrodynamic homology*, which is based on the scaling relations linking the hydrodynamic characteristics of each other and/or the molar mass. The fulfillment of such relations would mean the macromolecules compared behave hydrodynamically similar to each other and would allow interpreting the experimental results based on a single hydrodynamic model. The *structural homology*—being the highest form of homology—automatically leads to *hydrodynamic homology*, whereas the latter does not necessarily grant the occurrence of the first one.

This result (Figure 6) also means that the shape and size of *hb*PEG macromolecules is not distorted significantly by certain "defects" in the structure of the copolymers. Note that computer modeling of the shape and size of randomly hyperbranched polymers in solution allows to conclude that random attachment of component parts produces a good model of regularly branched polymers, i.e., dendrimers.[18] It supports the conclusion that the size and shape of ideal dendrimers and dendrimer molecules of higher generations in solution, with few structural defects, are virtually indistinguishable.[70,71] Thus, it follows from Figure 6 that glycogen as a hyperbranched biopolymer, perfectly branched dendrimers, the hyperbranched *hb*PEG studied in this contribution and globular proteins, despite their different chemical structures and fine topology, are *hydrodynamic homologues*. For these polymers a direct proportionality between the volume occupied by such macromolecules in solution and their masses is observed. It is the main feature of these systems. As a consequence, the intrinsic viscosity is independent of the molar mass for such

DOI: 10.1021/acs.macromol.5b01020
Macromolecules XXXX, XXX, XXX−XXX

homologous series, while the velocity sedimentation coefficient becomes more dependent on the molar mass which, in turn, provides advantages to the study of such systems by AUC.

From Figure 6 it is possible to determine the scaling relation between the value of the intrinsic viscosity and molar mass: $[\eta] = K_\eta M^{b\eta}$. A similar scaling relation or Kuhn−Mark−Houwink−Sakurada (KMHS) relationship/plot can be set for other hydrodynamic characteristics. Double-logarithmic KMHS scaling plots for samples in water are shown in Figure 7 (the scaling

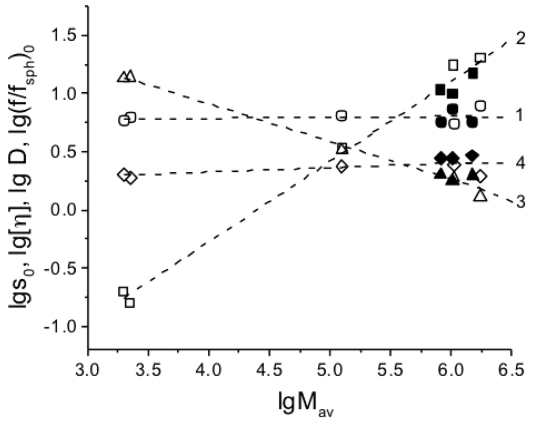

Figure 7. Dependencies of $[\eta]$ (1), s_0 (2), D (3), and $(f/f_{sph})_0$ (4), in a double-logarithmic plot, on the average molar mass M_{av} of hbPEG in H_2O. The scaling indexes are summarized in Table 4. Filled symbols are related to the samples with bimodal or highly broad molar mass distribution. It is evident that these data do not violate the general trend of the dependencies.

plots in DMF are presented in Supporting Information Figure 3, and the parameters of the KMHS relations are summarized in Table 4). In spite of the high heterogeneity of the studied *hb*PEGs (broad molar mass distributions, in some cases bimodal), all samples behave similarly and linear trends of KMHS relationships were obtained. A satisfactory correlation between the scaling indices b_i is observed within the error of their determination.

All our sets of hydrodynamic data indicate that the friction elements considered (isolated macromolecules) are similar with respect to their hydrodynamic behavior to globular-like particles with virtually constant degree of asymmetry. This conclusion is supported by the values of the scaling indices obtained from the double-logarithmic plots of the hydrodynamic characteristics vs molar mass. Thus, the macromolecules of the hyperbranched PEG copolymer follow the scaling relationships of the KMHS type, and the usual correlation between the scaling indices b_i is observed. In this approach, the series of the *hb*PEG copolymers may be considered as a hydrodynamically homologous series. Values of b_i as observed are characteristic of series of molecules/particles, which keep their form and asymmetry constant, going from low to high M. An example of a model that satisfies these conditions is a set of ellipsoids (spheroids) with a constant asymmetry. The simplest example of such a model is a series of hard spheres.

Comparison of the Retention Volume in SEC with Other Hydrodynamic Characteristics. In the ideal SEC (without adsorption contribution), molecules are separated according to their hydrodynamic volume. The well-known Benoit universal calibration curve connects the hydrodynamic volume, expressed as $[\eta]M$, with the retention volume V_R and can be used for molar mass estimation; however, the intrinsic viscosity must be known:

$$\log[\eta]M = C_1 - C_2 V_R \tag{10}$$

where C_1 and C_2 are constants characterizing the columns.

Figure 6 aids in understanding the results obtained by SEC and the discrepancy between M_{sD} and M_{SEC}. In accordance with relation 10, each value of the retention volume corresponds to the hydrodynamic volume of macromolecules contained in a portion of eluent sorted from the column. Thus, any line parallel to the X-axis corresponds to a retention volume. Such a line parallel to the X-axis intercepts first line **2** corresponding to linear PEG at low M and then line **1** corresponding to *hb*PEG at higher M. The difference between M_{sD} and M_{SEC} increases with increasing molar mass and/or with decreasing V_R so far as the slope of line **1** is lower than that of line **2**.

It has been shown previously that similar calibration curves can as well be applied for other hydrodynamic characteristics or their combinations and in the general case can be written as

$$\log[f(\langle R\rangle^2)] = C_i + C_{i+1} V_R \tag{11}$$

where $f(\langle R\rangle^2)$ is a function of the chain size and/or a combination of the experimental values which depend solely on the chain size, for instance, $[\eta]M$, $s_0[\eta]$, D_0, M/s_0, k_sM, and C_{i+1} are the coefficients of different sign.[74] In Figure 8 the dependencies of $\log(s_0[\eta])$, D, and $[\eta]M$ on V_{Ret} are shown; the parameters of the corresponding linear approximation procedures are listed in Supporting Information Table 2. This kind of plot allows to convert the macroscopic value of the retention volume to the nanoscale value of the hydrodynamic size of the macromolecules moving through the column.

Average Density of the Polymer in the Volume Occupied by Individual Macromolecules in Solution. The average density of the hyperbranched macromolecules in the volume occupied by them can be calculated based on the hydrodynamic characteristics for both branched and linear PEGs.[64] Using the

Table 4. Parameters of the KMHS Relationships for Hyperbranched PEG Copolymers in Water and DMF at 20 °C

	$b_i \pm \Delta b_i$		K_i		r_i	
P_i−M[a]	water	DMF	water	DMF	water	DMF
s_0	0.69 ± 0.03	0.65 ± 0.03	9.34×10^{-4}	2.08×10^{-3}	0.9959	0.9944
$[\eta]$	0.01 ± 0.02	0.02 ± 0.01	5.67	4.70	0.1830	0.6333
D_0	−(0.32 ± 0.02)		159		0.9931	
$(f/f_{sph})_0$	0.04 ± 0.02	0.01 ± 0.05	1.48	1.80	0.6454	0.0702

[a]The properties P_i of all the samples are related by $\log P_i = \log K_i + b_i \log M$; r_i is the corresponding linear correlation coefficient. Taking into account experimental errors, it can be seen that the scaling indices b_i are related to each other in the characteristic ways of a hydrodynamic homologous series of polymers: $|b_{D_0}| = (1 + b_{[\eta]})/3$; $|b_{D_0}| + b_{s_0} = 1$, $|b_{D_0}| = b_{ff} + 0.333$.

DOI: 10.1021/acs.macromol.5b01020
Macromolecules XXXX, XXX, XXX−XXX

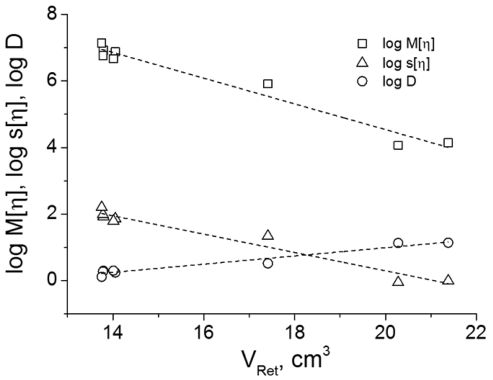

Figure 8. Universal calibration plots of log $M[\eta]$, log $s[\eta]$, and log D versus retention volume V_R in DMF. The scaling indexes are summarized in Supporting Information Table 2.

equivalent sphere approximation, the following relationships are obtained:

$$\rho_{sD} = 3^4 2\pi^2 k_B^{-2}[s][D]^2; \quad \rho_\eta = 2.5/[\eta] \tag{12}$$

The data for the calculations on linear PEG were taken from the literature, and the corresponding densities were calculated according to the following equations:[52,74]

$$\rho_{sD} = P^3 k_B^{-2}(0.36)^{-1}[s][D]^2; \quad \rho_\eta = \Phi/N_A 0.36[\eta] \tag{13}$$

where P and Φ are the Flory hydrodynamic parameters. The dependency of the calculated average density values (in water) on molar mass is presented in Figure 9 in double-logarithmic

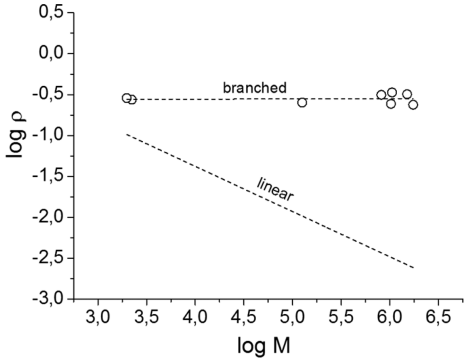

Figure 9. Dependence of the density of the polymer substance in the volume limited by the polymer coil (ρ) on the polymer mass (M) in double-logarithmic scale, for linear and *hb*PEGs in water. The corresponding scaling relationships are the following: $\rho = 6.8M^{-0.55\pm0.01}$ and $\rho = 0.27M^{0.00\pm0.02}$ for linear PEG and hyperbranched PEG copolymers, respectively.

scale. For the hyperbranched molecules, at the highest molar mass the density of the polymer substance in the polymer coil is approximately 70 times higher than for the linear chains. Furthermore, for the hyperbranched chains the density is virtually independent of the molar mass, while for linear macromolecules it decreases with the molar mass. The average densities are $\rho_\eta = 0.40 \pm 0.02$ and 0.41 ± 0.02 g cm^{-3} in water and DMF, respectively, and $\rho_{sD} = 0.21 \pm 0.01$ and 0.3 ± 0.1 g cm^{-3} in water and DMF, respectively. These values are comparable with or similar to those obtained for dendrimers based on poly(amidoamine), poly(propyleneimine), and perfectly branched dendrimers based on α-amino acids.[64,65,75]

Sizes and Branching Factors of hbPEG. The degree of branching is an important parameter for the hydrodynamic volume of the macromolecule: the higher the degree of branching, the smaller the size (as compared to linear macromolecules of the same molar mass). The effect of branching on the hydrodynamic volume of branched macromolecules can be characterized by the so-called shrinking or contraction factor, which is the ratio of the hydrodynamic characteristics and/or the mean square of the radius of gyration of the branched macromolecule and its linear analogueon of the same molar mass. These parameters were first introduced by Zimm and Stockmayer for the radius of gyration and then by Stockmayer and Fixman for the intrinsic viscosity. A similar relation can also be written for the translation friction coefficients g' and h:[20,21]

$$g' = \frac{[\eta]_b}{[\eta]_{lin}}; \quad h = \frac{f_b^t}{f_{lin}^t} \tag{14}$$

The data on the intrinsic viscosity and translational friction coefficient (calculated from the corresponding diffusion coefficients) for linear PEGs can be taken from the literature ($[\eta] = 0.133M^{0.59}$, $D = 940M^{-0.53}$).[74] The size can directly be represented either by the hydrodynamic radius (R_D, R_s, and R_η) or by the mean-square radius of gyration $\langle R_g^2 \rangle$. The molecular sizes were calulated using the following relationships:

$$R_D = \frac{k_B T}{6\pi\eta_0 D}; \quad R_s = \frac{3}{\sqrt{2}}\sqrt{[s]v}; \quad R_\eta = \left(\frac{3}{10\pi N_A}\right)^{1/3}(M[\eta])^{1/3} \tag{15}$$

The calculated values of the hydrodynamic radii for *hb*PEG in water and DMF are summarized in Supporting Information Table 3. The hydrodynamic sizes increase with molar mass, reaching a maximum value of about 14 nm for the highest molar mass sample 8. The values of the contraction factors (g' and h) are summarized in Table 5. As expected, contraction

Table 5. Correlation Parameters of the Contraction Factors g' and h of the HbPEG with the Molar Masses and between Them

$G_i - G_j$[a]	$b_{ij} \pm \Delta b_{ij}$	$K_{ij} \pm \Delta K_{ij}$	r_{ij}
$g' - M$	$-(0.58 \pm 0.02)$	44 ± 3	0.9929
$h - M$	$-(0.20 \pm 0.01)$	5.8 ± 0.5	0.9705
$g' - h$	2.75 ± 0.20	0.30 ± 0.04	0.9831

[a]The contraction factor G_i of all the samples are related by $\log G_i = \log K_i + b_i \log M$ or $\log G_i = \log K_{ij} + b_{ij} \log G_j$, and r_{ij} is the corresponding linear correlation coefficient.

factors decrease with increasing molar mass, reflecting higher segment density. The molar mass dependence of these parameters is presented in Supporting Information Table 4.

The relation between g' and h for branched macromolecules was first proposed by Stockmayer and Fixman based on the Kirkwood–Riseman theory. It was shown that g' could be evaluated from the approximation

$$g' \cong h^3 \tag{16}$$

which means that the differences in solvent draining between the linear and branched molecular chains, when included into their corresponding mean size, can describe both the frictional coefficient and the intrinsic viscosity.[25] The double-logarithmic dependence g' vs h is presented in Supporting Information

DOI: 10.1021/acs.macromol.5b01020
Macromolecules XXXX, XXX, XXX−XXX

Figure 4, and the corresponding relation was obtained as $g' = 0.30h^{2.75\pm0.20}$. In addition, some considerations regarding the indirect estimation of the radius of gyration and the evaluation of corresponding branching factor are presented in the Supporting Information.

Global Conformation of the hbPEG Macromolecules. The experimental data obtained for the series of *hb*PEG copolymers in solution can be summarized as follows: (i) the values of the intrinsic viscosity are small and almost independent of molar mass, (ii) the values of the sedimentation coefficients are high and strongly dependent on the molar mass of the samples, and (iii) the translational frictional coefficients are markedly dependent on the molar mass of the samples. In addition, higher Huggins parameter values and also higher values of the parameter $k_s/[\eta]$ are observed, as compared with the values characteristic for linear chains. All this suggests that the macromolecules studied are compact nano-objects, characterized by a high average density of the polymer material in the volume occupied by them. For instance, the average value of the intrinsic viscosity of the *hb*PEG copolymer samples are $[\eta] = 6.3 \pm 0.3$ cm^3 g^{-1} in H_2O and $[\eta] = 6.4 \pm 0.4$ in DMF, which is only 3 times higher than for the rigid sphere limit: $[\eta]_{sph} = 2.5\upsilon$, which in our case will be $[\eta]_{sph} \approx 2.0$ cm^3 g^{-1} in both solvents. The organization of the poly(ethylene glycol)-*co*-poly(glycerol)s can be described by a soft spheroid partially permeable for the solvent molecules. Modeling of the macromolecules in solution by rigid bodies, as performed earlier, nowadays is being replaced by the simulation of macromolecules by soft bodies.[76,77] Such mathematical modeling is implemented using a coarse-grained modeling concept.[78,79] The coarse-grained model (or "blob model") represents a macromolecule as a whole in the form of a soft body, the radius of which is equal to its radius of gyration and is allowed to fluctuate. Different soft-body models were considered for different types of polymers.[80,81] The direct application of a coarse-grained model, and its straightforward comparison with the experimental results currently is not possible.

In general, the value of the intrinsic viscosity of the hyperbranched polymers may be represented as $[\eta] = \nu(p,h,\varepsilon)\overline{\upsilon}$, where $\nu(p,h,\varepsilon)$ is a dimensionless coefficient depending on the asymmetry p of the soft body modeling of any macromolecule, on the thickness of the corona h accessible for the solvent molecules, and on the thermodynamic quality of the solvent (ε). A significant part of the energy loss due to friction of any macromolecule in solution is contributed by the external layers. Some attempts to obtain a theoretical expression for the intrinsic viscosity of the soft sphere depending on the thickness of the layer available for the solvent molecules may be found in the literature.[82,83] However, the present state of theory does not allow for the interpretation of experimental data on the intrinsic viscosity of soft macromolecules.

The influence of draining effects on the value of the intrinsic viscosity of spheres has been demonstrated by the Debye–Bueche theory for a model of a rigid sphere permeable for the solvent molecules.[84] The value of $[\eta]$ for the uniformly permeable sphere was found to be 3.6 times higher than that for the impermeable one. The solution behavior of the *hb*PEG macromolecules can be described by soft spheroids with some asymmetry and with partial draining by the solvent molecules. Separating the contributions to the small value of $[\eta]$ due to the draining effect on one side and to molecular asymmetry on the other side is currently not possible. The main result obtained in this study on the *hb*PEG copolymers is to establish a scaling relation, which is typical for a series of the macromolecules characterized by direct proportionality between molar mass and volume of the macromolecules/species. (The simplest case of such series is a series of rigid spheres.) This allows us to consider the studied set of *hb*PEG copolymers as a hydrodynamically homologous series.

CONCLUSIONS

To the best of our knowledge, this study represents the first combined approach of analytical ultracentrifugation, intrinsic viscosity, translational diffusion measurements, and SEC to a long-standing challenge, i.e., absolute molar mass determination of hyperbranched polymers. The one-step synthesis of hyperbranched poly(ethylene glycol)-*co*-poly(glycerol)s (*hb*PEG) copolymers based on random anionic ring-opening copolymerization of ethylene oxide with a minor fraction of glycidol as a branching agent has been further developed to generate a variety of molar masses. Biocompatible materials with multiple hydroxyl functionalities are obtained by this strategy. A series of copolymers with moderate polydispersity ($M_w/M_n \approx 2.1$) were obtained, with varying glycerol content (7–64 mol %, DB = 0.04–0.54) and molar masses from 1400 to 1 700 000 g mol^{-1}, depending on the solvent employed for the synthesis. The randomly branched structure of the copolymers was confirmed by ^{1}H and ^{13}C NMR spectroscopy. Absolute molar mass characterization still represents a major challenge for hyperbranched polymers in general. This study aims at this issue using molecular hydrodynamic methods in dilute solution, showing that the isolated macromolecules follow the scaling relationships with scaling indices characteristic of particles with constant asymmetry. Remarkably, the intrinsic viscosity of the *hb*PEG polymers virtually does not depend on molar mass ($[\eta] \sim M^{\approx 0}$); on the other hand, the sedimentation velocity coefficients strongly depend on molar mass ($s_0 \sim M^{0.69}$). The solution behavior of the *hb*PEG macromolecules can be qualitatively described by soft spheroids with some degree of draining and unknown asymmetry. Based on their hydrodynamic behavior and based on the average coil density, the *hb*PEG macromolecules in solution can be viewed to some extent as a dendrimer or globular-like systems. Furthermore, the value of the partial specific volume of the copolymer molecules correlates with the content of glycerol component, which confirms the degree of branching (DB) and may be used to estimate the DB. The retention volumes of the samples in SEC analysis correlate reasonably with other experimental hydrodynamic values characterizing the size of the macromolecules. Hydrodynamic radii of up to 14 ± 1 nm in aqueous solution suggest that the hyperbranched PEGs prepared in dioxane might be the largest synthetic hyperbranched structures reported to date.

ASSOCIATED CONTENT

Supporting Information

The Supporting Information is available free of charge on the ACS Publications website at DOI: 10.1021/acs.macromol.5b01020.

Figures 1–4 and Tables 1–4 (PDF)

DOI: 10.1021/acs.macromol.5b01020
Macromolecules XXXX, XXX, XXX–XXX

AUTHOR INFORMATION

Corresponding Authors

*E-mail hfrey@uni-mainz.de (H.F.).
*E-mail ulrich.schubert@uni-jena.de (U.S.S.).
*E-mail georges.pavlov@pobox.spbu.ru (G.M.P.).

Notes

The authors declare no competing financial interest.

ACKNOWLEDGMENTS

The authors are grateful to the Thuringia Ministry for Education, Science, and Culture (grant #B514-09051, Nano-ConSens) and to the Carl-Zeiss Stiftung (Strukturantrag JCSM) for financial support. We thank Prof. Dr. Dieter Schubert for helpful comments on the manuscript.

REFERENCES

(1) Flory, P. J. *J. Am. Chem. Soc.* **1941**, *63* (11), 3083−3090.
(2) Tomalia, D. A.; Naylor, A. M.; Goddard, W. A. *Angew. Chem., Int. Ed. Engl.* **1990**, *29* (2), 138−175.
(3) de Brabander-van den Berg, E. M. M.; Meijer, E. W. *Angew. Chem., Int. Ed. Engl.* **1993**, *32* (9), 1308−1311.
(4) Newkome, G. R.; Moorefield, C. N.; Vogtle, F. *Dendritic Molecules: Concepts, Syntheses, Perspectives*; Wiley-VCH: Weinheim, 1996.
(5) Carlmark, A.; Hawker, C.; Hult, A.; Malkoch, M. *Chem. Soc. Rev.* **2009**, *38* (2), 352−362.
(6) Gao, C.; Yan, D. *Prog. Polym. Sci.* **2004**, *29* (3), 183−275.
(7) Inoue, K. *Prog. Polym. Sci.* **2000**, *25* (4), 453−571.
(8) Segawa, Y.; Higashihara, T.; Ueda, M. *Polym. Chem.* **2013**, *4* (6), 1746−1759.
(9) Voit, B. I.; Lederer, A. *Chem. Rev.* **2009**, *109* (11), 5924−5973.
(10) Dong, R.; Zhou, Y.; Zhu, X. *Acc. Chem. Res.* **2014**, *47*, 2006.
(11) Knop, K.; Pavlov, G. M.; Rudolph, T.; Martin, K.; Pretzel, D.; Jahn, B. O.; Scharf, D. H.; Brakhage, A. A.; Makarov, V.; Mollmann, U.; Schacher, F. H.; Schubert, U. S. *Soft Matter* **2013**, *9*, 715−726.
(12) Sunder, A.; Heinemann, J.; Frey, H. *Chem. - Eur. J.* **2000**, *6* (14), 2499−2506.
(13) Wei, Z.; Hao, X.; Kambouris, P. A.; Gan, Z.; Hughes, T. C. *Polymer* **2012**, *53* (7), 1429−1436.
(14) Konkolewicz, D.; Monteiro, M. J.; Perrier, S. B. *Macromolecules* **2011**, *44* (18), 7067−7087.
(15) Hult, A.; Johansson, M.; Malmström, E. Hyperbranched Polymers. In *Branched Polymers II*; Roovers, J., Ed.; Springer: Berlin, 1999; Vol. *143*, pp 1−34.
(16) Schüll, C.; Rabbel, H.; Schmid, F.; Frey, H. *Macromolecules* **2013**, *46* (15), 5823−5830.
(17) Sunder, A.; Hanselmann, R.; Frey, H.; Mülhaupt, R. *Macromolecules* **1999**, *32* (13), 4240−4246.
(18) Konkolewicz, D.; Gilbert, R. G.; Gray-Weale, A. *Phys. Rev. Lett.* **2007**, *98* (23), 238301.
(19) Konkolewicz, D.; Perrier, S.; Stapleton, D.; Gray-Weale, A. *J. Polym. Sci., Part B: Polym. Phys.* **2011**, *49* (21), 1525−1538.
(20) Zimm, B. H.; Stockmayer, W. H. *J. Chem. Phys.* **1949**, *17* (12), 1301−1314.
(21) Stockmayer, W. H.; Fixman, M. *Ann. N. Y. Acad. Sci.* **1953**, *57* (4), 334−352.
(22) Kurata, M.; Fukatsu, M. *J. Chem. Phys.* **1964**, *41* (9), 2934−2944.
(23) Kurata, M.; Abe, M.; Iwama, M.; Matsushima, M. *Polym. J.* **1972**, *3* (6), 729−738.
(24) Li, L.; Lu, Y.; An, L.; Wu, C. *J. Chem. Phys.* **2013**, *138* (11), 114908.
(25) Burchard, W. Solution Properties of Branched Macromolecules. In *Branched Polymers II*; Roovers, J., Ed.; Springer: Berlin, 1999; Vol. *143*, pp 113−194.
(26) Wilms, D.; Schömer, M.; Wurm, F.; Hermanns, M. I.; Kirkpatrick, C. J.; Frey, H. *Macromol. Rapid Commun.* **2010**, *31* (20), 1811−1815.
(27) Zalipsky, S.; Harris, J. M. *Poly(ethylene glycol)*; American Chemical Society: Washington, DC, 1997; Vol. *680*, p 508.
(28) Knop, K.; Hoogenboom, R.; Fischer, D.; Schubert, U. S. *Angew. Chem., Int. Ed.* **2010**, *49* (36), 6288−6308.
(29) Dingels, C.; Schömer, M.; Frey, H. *Chem. Unserer Zeit* **2011**, *45* (5), 338−349.
(30) Kainthan, R. K.; Janzen, J.; Levin, E.; Devine, D. V.; Brooks, D. E. *Biomacromolecules* **2006**, *7* (3), 703−709.
(31) Wilms, D.; Stiriba, S.-E.; Frey, H. *Acc. Chem. Res.* **2010**, *43* (1), 129−141.
(32) Schömer, M.; Frey, H. *Macromol. Chem. Phys.* **2011**, *212* (22), 2478−2486.
(33) Lee, S.-I.; Schömer, M.; Peng, H.; Page, K. A.; Wilms, D.; Frey, H.; Soles, C. L.; Yoon, D. Y. *Chem. Mater.* **2011**, *23* (11), 2685−2688.
(34) Hawker, C. J.; Chu, F.; Pomery, P. J.; Hill, D. J. T. *Macromolecules* **1996**, *29* (11), 3831−3838.
(35) Dimitrov, P.; Hasan, E.; Rangelov, S.; Trzebicka, B.; Dworak, A.; Tsvetanov, C. B. *Polymer* **2002**, *43* (25), 7171−7178.
(36) Feng, X.-S.; Taton, D.; Chaikof, E. L.; Gnanou, Y. *J. Am. Chem. Soc.* **2005**, *127* (31), 10956−10966.
(37) Feng, X.; Taton, D.; Chaikof, E. L.; Gnanou, Y. *Macromolecules* **2009**, *42* (19), 7292−7298.
(38) Pang, Y.; Liu, J.; Wu, J.; Li, G.; Wang, R.; Su, Y.; He, P.; Zhu, X.; Yan, D.; Zhu, B. *Bioconjugate Chem.* **2010**, *21* (11), 2093−2102.
(39) Cao, H.; Dong, Y.; O'Rorke, S.; Wang, W.; Pandit, A. *Nanotechnology* **2011**, *22* (6), 065604.
(40) Walach, W.; Trzebicka, B.; Justynska, J.; Dworak, A. *Polymer* **2004**, *45* (6), 1755−1762.
(41) Lapienis, G.; Penczek, S. *Macromolecules* **2000**, *33* (18), 6630−6632.
(42) Lapienis, G.; Penczek, S. *J. Polym. Sci., Part A: Polym. Chem.* **2004**, *42* (7), 1576−1598.
(43) Unal, S.; Lin, Q.; Mourey, T. H.; Long, T. E. *Macromolecules* **2005**, *38* (8), 3246−3254.
(44) Schömer, M.; Schüll, C.; Frey, H. *J. Polym. Sci., Part A: Polym. Chem.* **2013**, *51* (5), 995−1019.
(45) Filippov, A.; Amirova, A. I.; Kirila, T.; Belyaeva, E. V.; Sheremetyeva, N. A.; Muzafarov, A. M. *Polym. Int.* **2015**, *64* (6), 780−786.
(46) Schuck, P. *Biophys. J.* **2000**, *78*, 1606−19.
(47) Maechtle, W.; Boerger, L. *Analytical Ultracentrifugation of Polymers and Nanoparticles*; Springer: Berlin, 2006.
(48) Tsvetkov, V. N. *Rigid Chain Polymers*; Plenum Press: New York, 1989.
(49) Kratky, O.; Leopold, H.; Stabinger, H. The determination of the partial specific volume of proteins by the mechanical oscillator technique. In *Methods in Enzymology*; Academic Press: New York, 1973; Vol. *27*, pp 98−110.
(50) Kainthan, R. K.; Muliawan, E. B.; Hatzikiriakos, S. G.; Brooks, D. E. *Macromolecules* **2006**, *39* (22), 7708−7717.
(51) Frey, H.; Hölter, D. *Acta Polym.* **1999**, *50*, 67−76.
(52) Brandrup, J.; Immergut, E. H.; Grulke, E. A. *Polymer Handbook*, 4th ed.; Wiley: New York, 1999.
(53) Rowe, A. J. *Biopolymers* **1977**, *16*, 2595−2611.
(54) Pyun, C. W.; Fixman, M. *J. Chem. Phys.* **1964**, *41* (4), 937−944.
(55) Wales, M.; Van Holde, K. E. *J. Polym. Sci.* **1954**, *14* (73), 81−86.
(56) Morawetz, H. *Macromolecules in Solution*, 2nd ed.; Wiley: New York, 1975.
(57) Tsvetkov, V. N.; Lavrenko, P. N.; Bushin, S. V. *J. Polym. Sci., Polym. Chem. Ed.* **1984**, *22* (11), 3447−3486.
(58) Pavlov, G. M.; Perevyazko, I. Y.; Okatova, O. V.; Schubert, U. S. *Methods* **2011**, *54*, 124−135.
(59) Pavlov, G. M.; Korneeva, E. V.; Nepogod'ev, S. A.; Jumel, K.; Harding, S. E. *Polymer Sci. Ser. A* **1998**, *40*, 1282.

DOI: 10.1021/acs.macromol.5b01020
Macromolecules XXXX, XXX, XXX−XXX

(60) Pavlov, G.; Korneeva, E.; Jumel, K.; Harding, S.; Meijer, E. W.; Peerlings, H. W. I.; Stoddart, J. F.; Nepogodiev, S. *Carbohydr. Polym.* **1999**, *38* (3), 195−202.
(61) Pavlov, G. M.; Korneeva, E. V.; Roy, R.; Michailova, N. A.; Ortega, P. C.; Perez, M. A. *Prog. Colloid Polym. Sci.* **1999**, *113*, 150−157.
(62) Pavlov, G. M.; Korneeva, E. V.; Michailova, N. A.; Roy, R.; Cejas Ortega, P.; Alamino Perez, M. *Vysokomol. Soedin., Ser. A* **1999**, *41*, 1810−1815.
(63) Pavlov, G. M.; Errington, N.; Harding, S. E.; Korneeva, E. V.; Roy, R. *Polymer Sci. Ser. A* **2001**, *43*, 118.
(64) Pavlov, G. M.; Errington, N.; Harding, S. E.; Korneeva, E. V.; Roy, R. *Polymer* **2001**, *42* (8), 3671−3678.
(65) Pavlov, G. M.; Korneeva, E. V.; Meijer, E. W. *Colloid Polym. Sci.* **2002**, *280* (5), 416−423.
(66) Pavlov, G.; Frenkel, S. *Prog. Colloid Polym. Sci.* **1995**, *99*, 101−108.
(67) Pavlov, G. M. *Eur. Phys. J. E: Soft Matter Biol. Phys.* **2007**, *22* (2), 171−80.
(68) Pavlov, G. Hydrodynamics of Macromolecules: Conformation Zoning for General Macromolecules. In *Encyclopedia of Biophysics*; Roberts, G. K., Ed.; Springer: Berlin, 2013; pp 1014−1024.
(69) Grubisic, Z.; Rempp, P.; Benoit, H. *J. Polym. Sci., Part B: Polym. Lett.* **1967**, *5* (9), 753−759.
(70) Mikhailov, I. V.; Darinskii, A. A. *Polym. Sci., Ser. A* **2014**, *56* (4), 534−544.
(71) Bessonov, V.; Balabaev, N.; Mazo, M. Influence of Branch Defect on Shape and Size of Dendrimers. In *5th International Symposium "Molecular Mobility and Order in Polymer Systems"*, St. Petersburg, Russia, 2005.
(72) Yanaki, T.; Norisuye, T.; Fujita, H. *Macromolecules* **1980**, *13* (6), 1462−1466.
(73) Sato, T.; Norisuye, T.; Fujita, H. *Macromolecules* **1984**, *17* (12), 2696−2700.
(74) Pavlov, G. M.; Korneeva, E. V.; Panarin, E. F. *J. Appl. Polym. Sci.* **1992**, *46* (11), 2059−2061.
(75) Vlasov, G. P.; Pavlov, G. M.; Bayanova, N. V.; Korneeva, E. V.; Ebel, C.; Khodorkovskii, M. A.; Artamonova, T. O. *Dokl. Phys. Chem.* **2004**, *399* (1−3), 290−292.
(76) Murat, M.; Kremer, K. *J. Chem. Phys.* **1998**, *108* (10), 4340−4348.
(77) Sheiko, S.; Möller, M. Hyperbranched Macromolecules: Soft Particles with Adjustable Shape and Persistent Motion Capability. In *Dendrimers III*; Vögtle, F., Ed.; Springer: Berlin, 2001; Vol. *212*, pp 137−175.
(78) D'Adamo, G.; Pelissetto, A.; Pierleoni, C. *Soft Matter* **2012**, *8* (19), 5151−5167.
(79) Zhang, G.; Daoulas, K. C.; Kremer, K. *Macromol. Chem. Phys.* **2013**, *214* (2), 214−224.
(80) Vettorel, T.; Besold, G.; Kremer, K. *Soft Matter* **2010**, *6* (10), 2282−2292.
(81) Eurich, F.; Karatchentsev, A.; Baschnagel, J.; Dieterich, W.; Maass, P. *J. Chem. Phys.* **2007**, *127* (13), 134905.
(82) Ohshima, H. *Langmuir* **2008**, *24* (13), 6453−6461.
(83) Mendoza, C. I. *J. Chem. Phys.* **2011**, *135* (5), 054904.
(84) Debye, P.; Bueche, A. M. *J. Chem. Phys.* **1948**, *16* (6), 573−579.

DOI: 10.1021/acs.macromol.5b01020
Macromolecules XXXX, XXX, XXX−XXX